Effect of Neodymium doping on the structural, morphological, optical and electrical properties of copper oxide thin films

Article *in* Journal of Materials Science Materials in Electronics · April 2018

DOI: 10.1007/s10854-018-9170-5

CITATIONS
0

READS
73

6 authors, including:

R. David Prabu
Arul Anandar College
7 PUBLICATIONS **10** CITATIONS
SEE PROFILE

S. Valanarasu
Arul Anandar College
67 PUBLICATIONS **329** CITATIONS
SEE PROFILE

Jegatha Jehinder
Jayaraj Annapackiam College for Women, periyakulam
10 PUBLICATIONS **126** CITATIONS
SEE PROFILE

Jeyadheepan Karu
SASTRA University
38 PUBLICATIONS **94** CITATIONS
SEE PROFILE

Some of the authors of this publication are also working on these related projects:

An effect of temperature on structural, optical, photoluminescence and electrical properties of copper oxide thin films deposited by nebulizer spray pyrolysis technique View project

Presently my team of researchers and I have started applying our knowledge to probe space and earth. Our current research interests are focussed on Soil, water and Gravity. Shortly we are exploring the needed insights for improving our understanding on the origin of universe. View project

Journal of Materials Science: Materials in Electronics
https://doi.org/10.1007/s10854-018-9170-5

Effect of Neodymium doping on the structural, morphological, optical and electrical properties of copper oxide thin films

R. David Prabu[1] · S. Valanarasu[1] · H. A. Herisalin Geno[2] · A. Jegatha Christy[2] · K. Jeyadheepan[3] · A. Kathalingam[4]

Received: 9 February 2018 / Accepted: 22 April 2018

Abstract
In the present work un-doped and neodymium (Nd)-doped copper oxide thin films were deposited using nebulizer spray pyrolysis technique. The XRD pattern confirmed, the Cu_2O phase for the films with cubic crystal structure. The calculated crystallite size of the Cu_2O thin films are 36, 34, 28, and 23 nm respectively for 0, 1, 3 and 5% of Nd doping level. In 5% Nd doping the voids were reduced and the film showed high absorption in the visible region due to the maximum thickness. The band gap values are 2, 1.94, 1.87 and 1.82 eV for the 0, 1, 3 and 5% of Nd respectively. The emission peak at ~ 617 nm was observed for all the films in PL spectra which corresponds to copper impurity of the deposited films. The low resistivity about 0.85×10^2 Ω cm was found for the 5% Nd doped copper oxide thin film. The open circuit voltage (V_{oc}) was 0.39 V and short circuit current (I_{sc}) was 1.1641×10^{-4} A for the 5% Nd doped Cu_2O thin film.

1 Introduction

The copper oxide thin films have fascinated great interest due to their considerable applications in many technological fields. Copper oxide is non toxic, abundant on earth, high absorption coefficient in the visible region, exhibits fairly high minority carrier diffusion lengths, and large exciton binding energy. The copper oxide thin films were used as an active layer in different types of solar cells and a passive layer in solar-selective surfaces. The copper oxide thin film has two stable oxides: cupric oxide (CuO) and cuprous oxide (Cu_2O). The copper oxide thin films are p-type semiconductors having a band gap of 1.2–1.9 eV with monoclinic crystal structure for CuO phase and band gap of 1.9–2.5 eV with cubic crystal structure for Cu_2O phase [1]. In the above mentioned oxides Cu_2O is mainly studied because of its fine electrical properties with high optical absorption coefficient in the visible range [2]. Copper oxide films have been deposited using several techniques such as electrodepositing [3], plasma evaporation [4], chemical vapour deposition [5], thermal oxidation [6], reactive sputtering [7], sol–gel [8], spray pyrolysis [9], nebulizer spray pyrolysis [10]. From the various thin film techniques that were mentioned above, nebulizer spray pyrolysis technique has been widely used due to its cost effective, facile and large production of metal oxide thin films. The advantage of nebulizer spray pyrolysis over conventional spray pyrolysis are as follows: (i) consumption of low materials (ii) low carrier gas pressure with high-quality spray control (iii) films with desired properties like pinhole free with homogeneous layer can be prepared. A fabulous attention has been paid for the doping of rare-earth materials because of their properties of antiseptic, immune modulatory, antineoplastic, anticoagulant and low toxicity [11, 12]. For the first time, rare earth material (Nd) is doped with copper oxide thin films using nebulizer spray pyrolysis. The effect of neodymium (Nd) on the structural, morphological, optical, electrical and photovoltaic properties were studied. The obtained results are discussed in this report.

✉ S. Valanarasu
valanroyal@gmail.com

[1] PG and Research Department of Physics, Arul Anandar College, Karumathur, Madurai, India

[2] Department of Physics, Jeyaraj Annapackiam College for Women, Periyakulam, Theni, India

[3] School of Electrical and Electronics Engineering, SASTRA University, Thanjavur 613401, India

[4] Millimeter-Wave Innovation Technology Research Center (MINT), Dongguk University, Seoul 04620, Republic of Korea

Published online: 30 April 2018

2 Experimental details

2.1 Preparation of precursor solution

Copper oxide thin films prepared by the nebulizer spray pyrolysis (NSP) technique was already discussed in the previous report [13]. For the preparation of Nd doped copper oxide thin film the copper(II) acetate monohydrate, glucose, 2-propanol and neodymium(III) acetate were taken. First of all copper(II) acetate monohydrate ($Cu(CO_2CH_3)_2{\cdot}H_2O$) and glucose ($C_6\ H_{12}\ O_6$) with 0.1 M was taken and were dissolved in double distilled water. The 2-propanol [$(CH_3)_2$ CHOH] of 20% volume is added to the precursor solution. The different % of neodymium (Nd $(O_2C_2H_3)_3\ H_2O$) (0, 1, 3 and 5%) are added to the above mentioned solution. The solution was stirred well for 30 min to form a homogeneous solution. The volume for each deposition was 10 mL. In the precursor solution, glucose was added which is a reducing agent [14]. The 2-propanol was added in to the solution in order to increase the wet-ability of the droplet to the substrate. It may reduce the surface tension of the prepared solution [15]. The glass substrate was maintained at a standardized temperature (i.e. 280 °C) maintained by extremely stable temperature controller by using thermocouple. The deposition parameters like temperature, molarity, solution volume and deposition pressure are already reported in the previous work [16, 17]. The distance between the substrate and the nozzle was kept at ~ 5 cm and the pressure was 3 bar. In order to get the crack free film, the film was allowed to cool at room temperature after the deposition was over.

For the preparation of ZnO/Nd:Cu_2O heterojunction, ZnO layer was coated onto the FTO by spraying 5 ml of zinc acetate with 0.1 M keeping the substrate at 400 °C and spray pressure of about 1 bar.

2.2 Characterization

The structural properties of the Nd doped Cu_2O films were analyzed by Bruker AXS D8 advance X-ray diffractometer using Cu Kα radiations (λ = 1.5406 Å). Scanning electron microscope was used to study the surface morphology of the deposited films by using Carl Zeiss evo' 18 fitted with an energy dispersive X-ray analysis (EDAX) with accessories. A profilometer was used to measure the thickness of the deposited Nd doped Cu_2O thin films. Optical studies were carried out using Perkin Elmer UV–Vis spectrometer (Hitatchi-330) in the wavelength region of 300–1100 nm. The Perkin Elmer LS55 fluorescence spectrophotometer with an excitation source from Xe lamp was used to measure the photoluminescence spectra of the deposited Nd doped Cu_2O thin films in the wavelength range of 400–900 nm. Hall effect measurement was used to study the electrical properties of the Nd doped copper oxide thin films with the use of four probe method. The Keithley source meter with the help of four probe were used to study the resistivity in the range of 30–200 °C. I–V characterization of the fabricated n-ZnO/p-Nd:Cu_2O heterojunction was done under 200 W/m^2 halogen lamp illuminated conditions. Ag paste was used as dots to take metal contact. The ohmic contact of the silver paste to the samples was checked with the IV measurements through all the four contacts and it showed the ohmic nature. Solar cell property of the constructed n-ZnO/p-Cu_2O heterojunction was studied using Keithley 4200 semiconductor parameter analyzer.

3 Result and discussion

3.1 Structural studies

The X-ray diffraction pattern of undoped and 1, 3 and 5% Nd doped copper oxide thin films were shown in Fig. 1. The observed diffraction peaks of the XRD pattern showed that the films are polycrystalline in nature having cubic

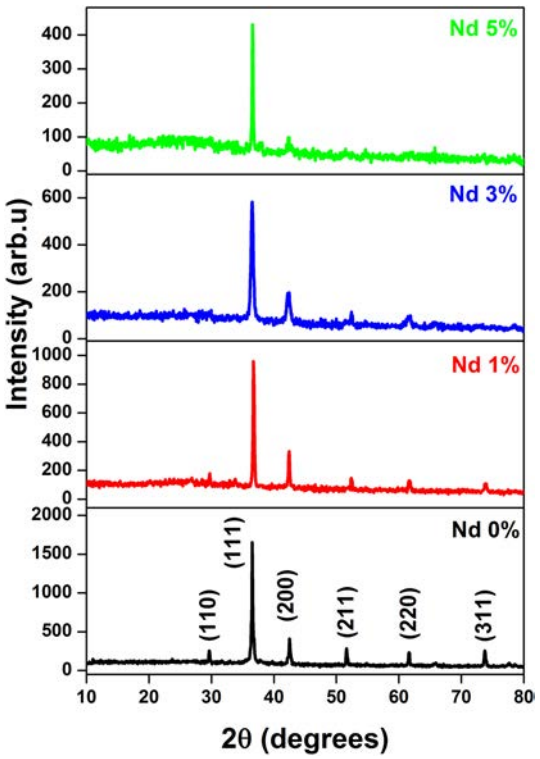

Fig. 1 XRD patterns of undoped and Nd-doped Cu_2O thin films

crystal structure and matched with JCPDS (Card No: 77-0199). The deposited Cu_2O thin films exhibited well defined peaks at 29.6°, 36.4°, 42.3°, 61.3°, and 73.7° corresponding to (110), (111), (200), (220) and (311) planes, respectively. In the XRD patterns no other phases such as Cu or CuO are found which confirmed that all the samples exist as main Cu_2O phase. The intensity of all planes were decreased with the increasing of Nd doping from 0 to 5% which indicates the shrinkage of crystalline size. No peaks were observed for the Nd in the XRD pattern which shows that the Nd^{3+} ions were interstitial position near the Cu sites into the Cu_2O lattice.

The crystalline size of the Nd doped Cu_2O thin films were calculated using the Scherer's formula [18]

$$D = \frac{0.9\lambda}{\beta \cos\theta} \tag{1}$$

where θ is the Bragg angle, β is the full-width at half-maximum (FWHM) value, and λ is the X-ray wavelength (1.5406 Å). The calculated crystallite size of the Cu_2O thin films are 36, 34, 28, and 23 nm respectively for the 0, 1, 3 and 5% of Nd doping. The obtained crystallite size decreased on increasing the doping concentration which related to strain. This was probably indicating that Nd dopant contributing to the change in crystallinity. The dislocation density (δ) and strain (ε) values are determined from the below equations [19].

$$\delta = \frac{1}{D^2} \tag{2}$$

$$\varepsilon = \frac{\beta \cos\theta}{4} \tag{3}$$

where β is the FWHM and D is the crystallite size of the XRD peak. The dislocation density and micro strain gives more information about structural properties and it was presented in Table 1. The strain values changed with Nd doping caused by point defects and crystallite size. The dislocation density and strain increased because of grain boundaries increases due to the decrease of the crystallite size with the Nd doping.

The texture coefficient were used to calculate the preferred orientation of the crystallites, TC (hkl), by the following formula [20]

$$TC(hkl) = \frac{I(hkl)/I_0(hkl)}{N_r^{-1}\sum I(hkl)/I_0(hkl)} \tag{4}$$

where, $I_{(hkl)}$ is the measured intensity, $I_{0(hkl)}$ is the standard intensity of the corresponding plane, TC is the texture coefficients of the (hkl) plane, and N is the number of reflection peaks. The predominant peak (111) in the X-ray diffraction pattern with high crystinallity was taken to obtain the values of texture coefficient. The observed value of the texture coefficient (TC > 1) was higher than 1 which indicates the preferential orientation and also point out the abundance of grains in the (hkl) direction. As the Nd doping increases the texture coefficient value decreases. The observed texture coefficient value is well matched with the previous result of Nagai et al. [21].

The Nd doped copper oxide thin films are having cubic crystal structure and the lattice parameter 'a' is calculated from the relation [22]. The hkl value of (111) and d-spacing were used to calculate the lattice parameters. The cell volume was calculated by using the formula of $V = a^3$ for the cubic crystal structure. The cell volume decreases with the increase of doping level. The lattice constant of the undoped film found to be a = 4.2599 Å, well matched with the standard values of JCPDS Card No 77-0199. The texture coefficient and cell volume values are tabulated in Table 2. The obtained cell volume value was well supported with the standard JCPDS (Card No 77-0199). The thicknesses of the films were measured by the use of profilometer and found to be 600, 640, 700, 780 nm respectively for the different (0, 1, 3 and 5%) of Nd doping level.

3.2 Morphological studies

Figure 2a–c showed SEM images of Nd doped Cu_2O films for un-doped and different % of Nd doping. All SEM images showed that the prepared films were cubic shaped particles and well uniform all over the surface. From the figure, cubic

Table 1 Structural parameters of copper oxide thin films

Nd doping (%) in Cu_2O	Thickness (nm)	Crystallite size (nm)	Dislocation density ($\times 10^{15}$ lines m^{-2})	Micro strain ($\times 10^{-2}$ line^{-2} m^{-4})
0	600	36	0.77	0.31
1	640	34	0.86	0.32
3	700	28	1.24	0.39
5	780	23	1.84	0.47

Table 2 Lattice parameters and TC values for Nd doped copper oxide thin films with reference JCPDS No: 77-0199

Nd doping (%) in Cu_2O	Texture coefficient (TC)	Lattice constant $a = b = c$ (Å)	Cell volume ($V = a^3$) $(Å)^3$
0	1.32	4.2599	77.30
1	1.28	4.2587	77.23
3	1.13	4.2574	77.16
5	1.07	4.2537	76.96

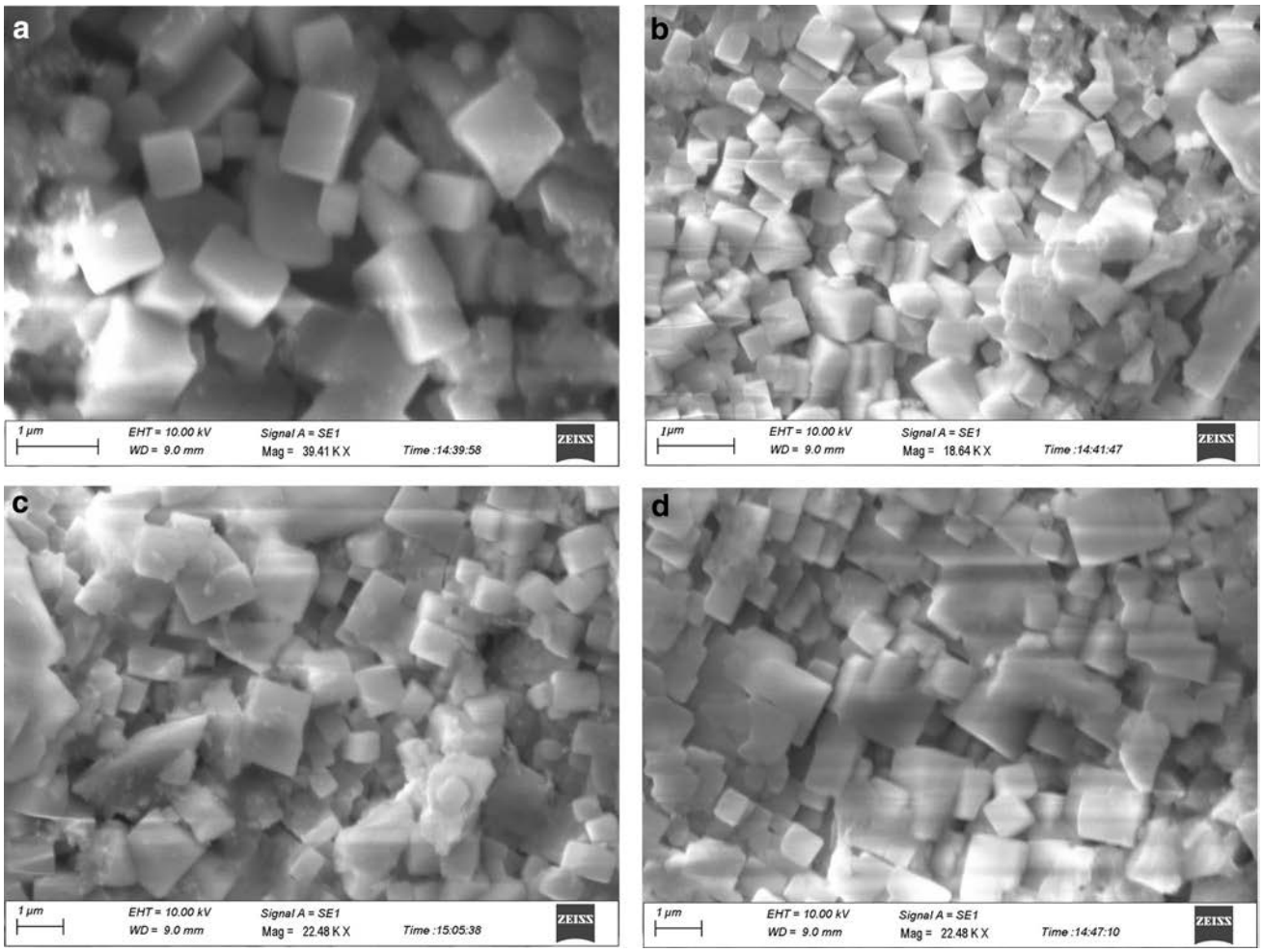

Fig. 2 SEM image of different **a** 0, **b** 1, **c** 3 and **d** 5% Nd doped Cu_2O films

shaped particles are uniformly arranged on the surface of deposited films, which was well matched with the standard cubic crystal structure of JCPDS (Card No: 77-0199). The observed cubic shaped particles are also matched with the previous result of Cu_2O SEM image by Khan et al. [23]. The Fig. 2a showed the particles are well arranged with some voids on the film surface. The voids were reduced when the Nd doping concentration (5%) was increased due to the Nd^{3+} ions occupying the porous nature of Cu_2O lattice. In addition the increased particles are uniformly arranged without any voids which suggest that Nd^{3+} ions were interstitial position near the Cu sites in the Cu_2O structure. As we see from the figures the size of the particle was changed with respect to Nd doping level due to the coalescence.

The 5% Nd doped Cu_2O thin film was analyzed by energy dispersive X-ray analysis (EDAX) technique for the compositional analysis and were showed in Fig. 3. The obtained peaks have confirmed the presence of copper, oxygen and Nd. The average atomic weight percentage ratio of Cu, O, and Nd in Cu: O: Nd thin film was 62.74 wt% : 34.04 wt%: 3.22 wt%. The presence of doped rare earth element Nd in Cu_2O thin film was confirmed by this analysis without any other impurities.

3.3 Optical studies

Figure 4 showed the optical absorption of the thin films examined at room temperature in the range of 300–1100 nm and clearly shown the samples have a maximum absorption in the range of 400–500 nm. The highest absorption at wavelength of 400–500 nm obtained for 5% Nd doped Cu_2O thin film is due to its maximum thickness amongst other films. The increase of film thickness explains the absorption of more photons on increasing the Nd doping %. Further, the structures become denser as the film thickness increased, which are confirmed by the obtained SEM images. The UV–Vis transmittance spectra of Cu_2O thin films which are shown in Fig. 5. The undoped Cu_2O thin film showed high transmittance in the visible region which confirmed that all the deposited films were sensitive to the film thickness.

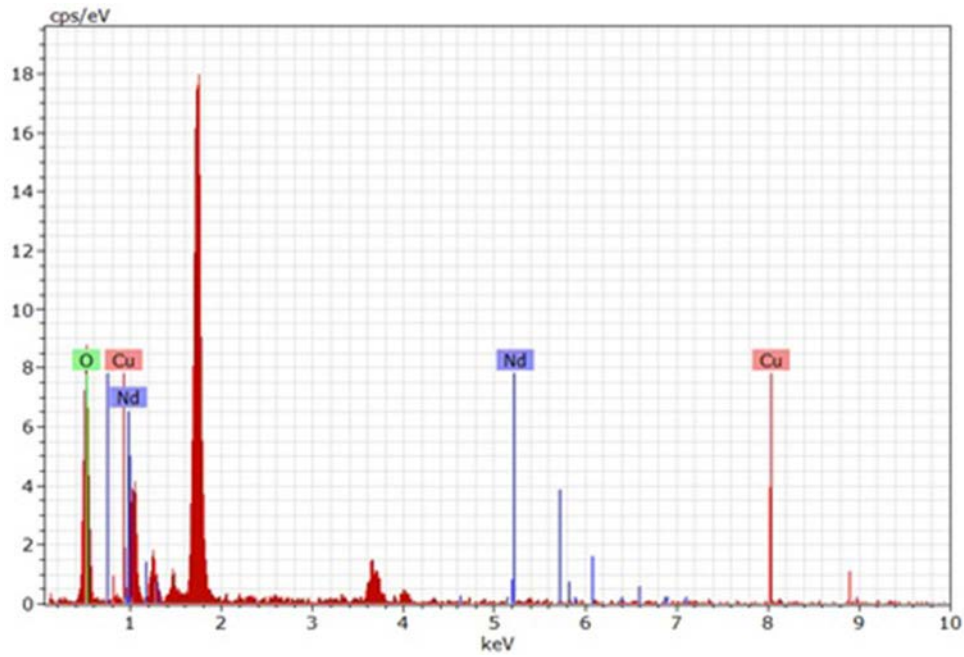

Fig. 3 EDAX spectra of 5% Nd doped Cu_2O thin film

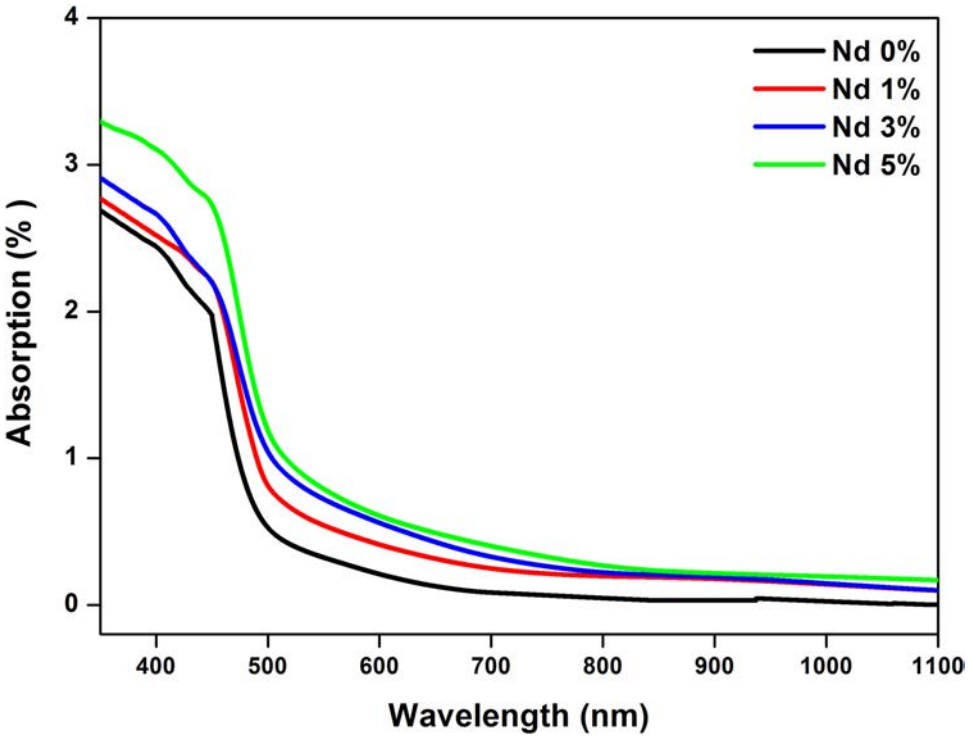

Fig. 4 Optical absorption spectra of undoped and Nd-doped Cu_2O thin films

The reflectance spectra shown in Fig. 6 with different % of Nd doping. The deposited films showed 16, 20, 27 and 33% reflectance for the 0, 1, 3 and 5% of Nd doping. The film deposited with 5% of Nd showed high reflectance due to the maximum thickness in the film.

The extrapolation techniques were used to determine optical band gap. The optical band gap was obtained by using the Tauc's formula [24]. The optical band gap values obtained by an extrapolation of the photon energy (hv) on the x-axis versus linear region of a plot of the graph of $(\alpha hv)^2$ on the y-axis. The band gap mainly depends on the observed red-shift (sharp absorption edge from the transmittance spectra) [23]. Figure 7 showed the optical band gap of different Nd doping %. It was observed that the optical band

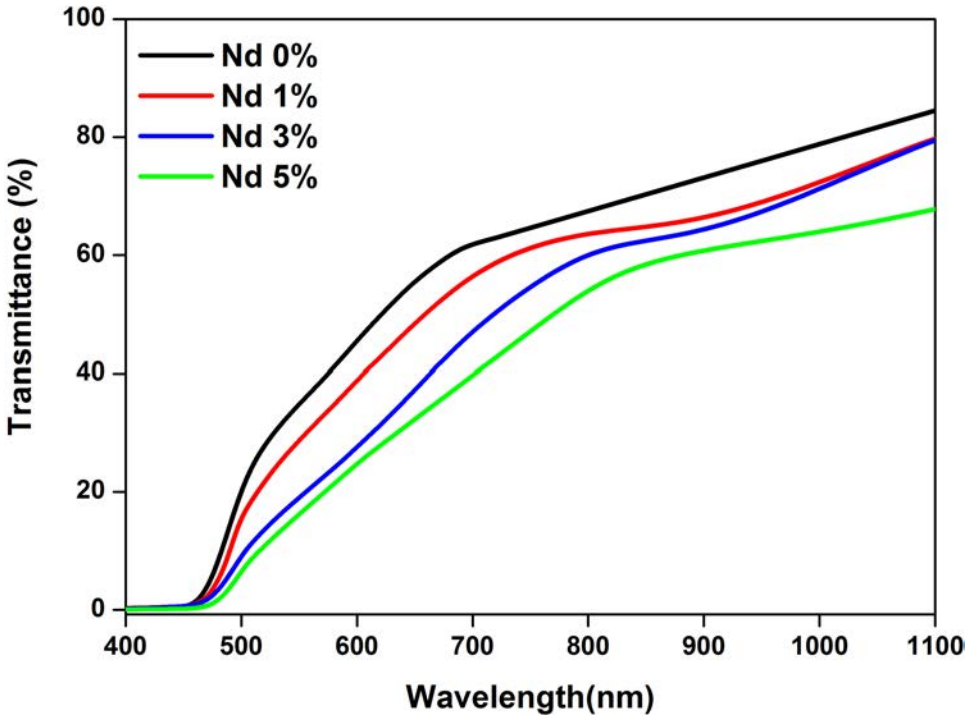

Fig. 5 Optical transmission spectra of undoped Nd-doped Cu_2O thin films

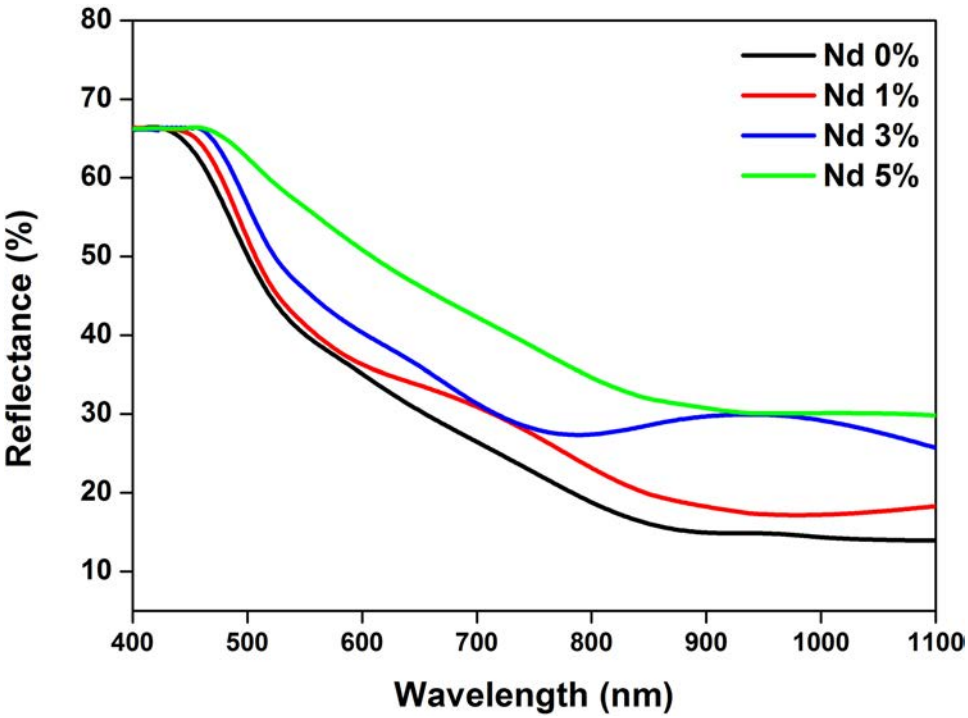

Fig. 6 Reflectance spectra of undoped Nd-doped Cu_2O thin films

gap decreased from 2, 1.94, 1.87 and 1.82 eV respectively for the increasing of Nd doping from 0 to 5%. In common, the band gap variations is directly proportional to the variations of crystallite size [25].

The refractive index (n) and extinction coefficient (k) were calculated by using the below Eq. (5, 6) respectively [26],

$$n = \left(\frac{1+R}{1-R}\right) + \sqrt{\frac{4R}{(1-R)^2} - K^2} \tag{5}$$

$$k = \frac{\alpha\lambda}{4\pi} \tag{6}$$

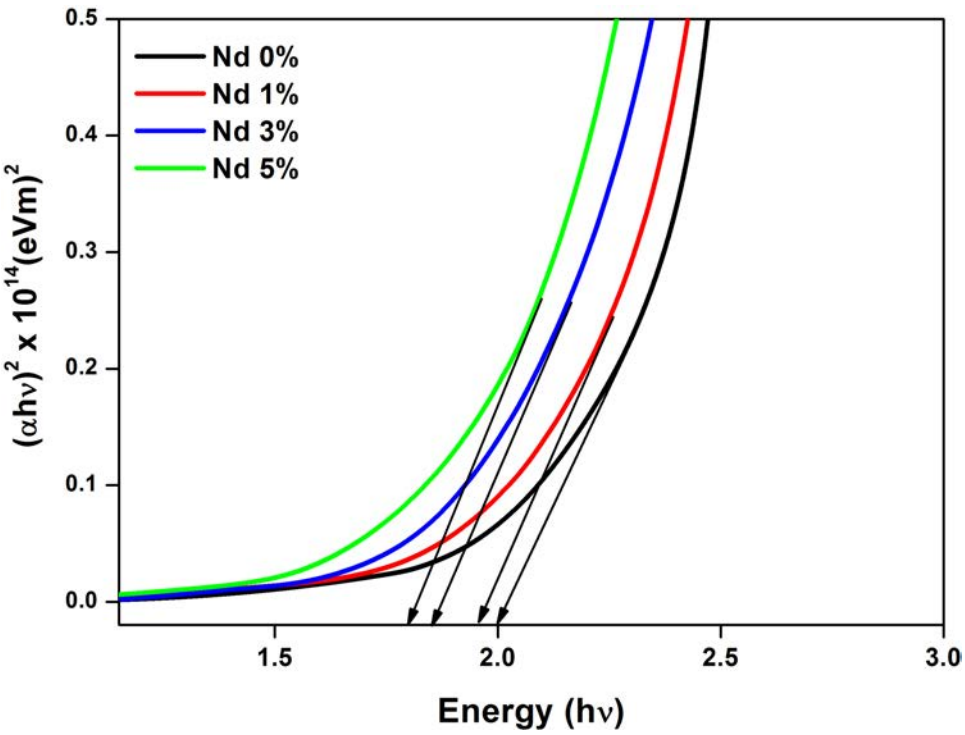

Fig. 7 Band gap curve of undoped Nd-doped Cu_2O thin films

Real (εr) and imaginary part (εi) of the dielectric constants were determined from Eqs. (8, 9 [25, 27]

$$\varepsilon = \varepsilon_1 + i\varepsilon_2 \tag{7}$$

$$\varepsilon_1 = n^2 - k^2 \tag{8}$$

$$\varepsilon_2 = 2nk \tag{9}$$

where, k is the extinction coefficient, n the refractive index of the material, ε_1 and ε_2 are real and imaginary part of dielectric constants, R is the reflectance (%) and λ is the wavelength in nm respectively. Figure 8 showed the refractive index (n) and extinction coefficient (k) of Cu_2O thin films deposited with different Nd doping concentration. The Refractive index value increased with the Nd doping, it was due to the film thickness. The high extinction coefficient values were found for the film deposited at the 5% Nd doping.

The real part of dielectric constant was found to be higher for the 5% Nd doped film, it was due to the favorable value of refractive index. The real part was related to the dispersion,

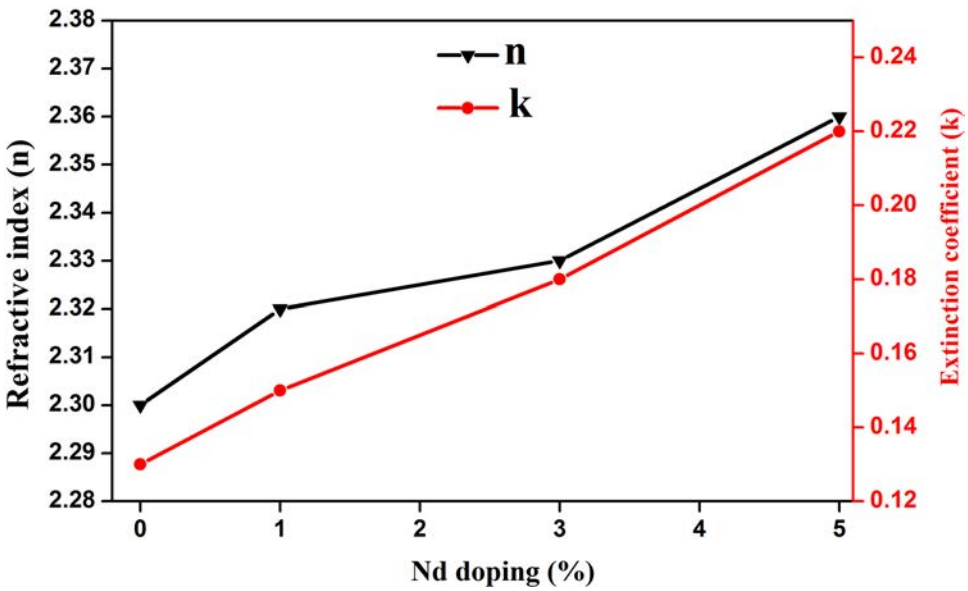

Fig. 8 Change of refractive index (n) and extinction coefficient (k) of Nd doped Cu_2O thin films with Nd doping concentration

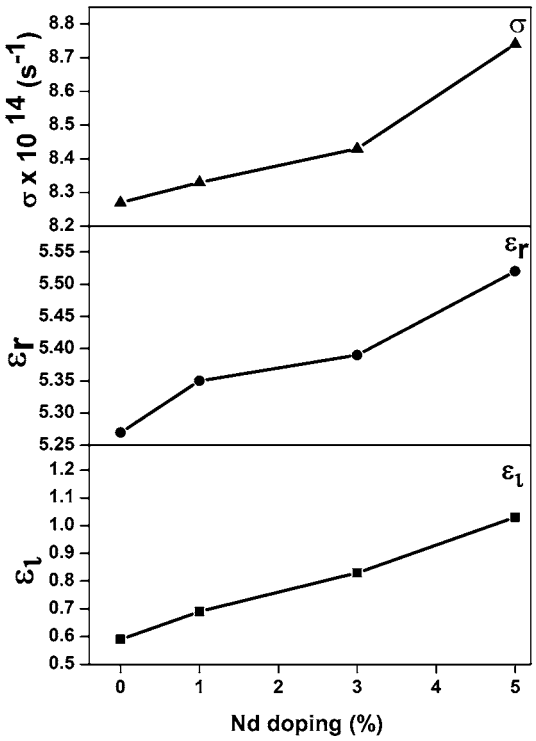

Fig. 9 Real, imaginary part of dielectric constant and optical conductivity of Cu_2O thin films for different Nd doping concentration

while the imaginary part estimated the dissipative rate of the wave in the medium.

The optical conductivity (σ) was d calculated using the below Eq. (10) [28],

$$\sigma = \alpha n c \tag{10}$$

where c is the velocity of light. The optical conductivity of the un-doped and Nd doped copper oxide thin films were shown in Fig. 9. The optical conductivity values at high photon energies appear enhanced due to the high absorbance [28].

3.4 PL spectra

To study the influence of Nd doping on the luminescence of Cu_2O film, we have measured at room-temperature PL spectra of Cu_2O films with different Nd doping %. Figure 10 shown the evolution of PL spectra at different Nd doping %. The PL spectra given an idea about the defect state. In general, the PL spectrum should have a broad defect related emission (DLE) in the visible region, occurs with the orange/red emission which was due to the radioactive transitions from defect sites related with the presence of excess of oxygen [29]. In our case, the observed emission peak at ~617 nm corresponds to copper impurity for all the copper oxide thin film. The PL emission at ~617 nm was observed

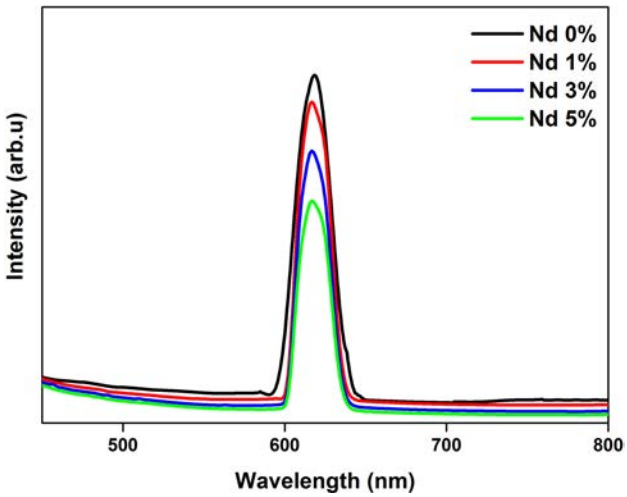

Fig. 10 PL spectra of undoped and Nd-doped Cu_2O thin films

for all the processed films, was due to near band-edge emission. Taking account of the band gap energy of Cu_2O, the PL peak was probably attributable to acceptor-related luminescence [30]. In Cu_2O films the observed peak at 617 nm is probably due to transitions between $^3\Gamma_5^+$ valence band and $^2\Gamma_7^+$ conduction band [29–31]. It is suggested that the Nd doping in copper oxide has an effect of decreasing a luminescence intensity of nano crystalline Cu_2O.

3.5 Electrical studies

Hall effect measurements were performed to characterize the electrical properties of un-doped and Nd doped copper oxide thin films. The deposited thin films were cut into 10 mm × 10 mm square and the conductive silver paste was placed at the diagonal edges of the samples, as prescribed by the ASTM standard F76-08. The ohmic contact of the silver paste to the samples was checked with the IV measurements through all the four contacts, prior to the Hall measurements. The effects of Nd doping on the electrical properties of Cu_2O thin films are shown in Fig. 11. The electrical properties of un-doped and Nd doped copper oxide thin film values are listed in Table 3. All the deposited copper oxide thin film shows the p-type conductivity. Copper vacancies in Cu_2O films acted as acceptors, causing p-type conduction. The hall mobility and carrier concentration were calculated using the Hall coefficient and the resistivity data. When the Nd doping increases, the resistivity decreased due to the increase in carrier concentration. For higher doping (5%), there was increase in thickness of the film which reduces the resistivity as there is an increase in the number of charge carriers. The resistivity value is 0.85×10^2 Ω cm for the 5% Nd doped Cu_2O thin film which is lower than the earlier report by spray pyrolysis technique [32]. The Hall mobility of Nd

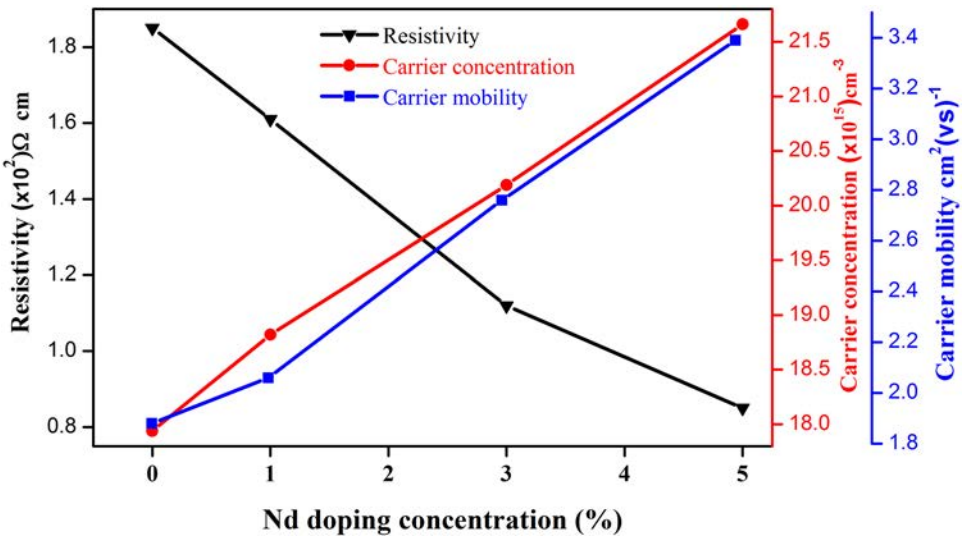

Fig. 11 Electrical resistively (ρ), carrier concentration (n) and carrier mobility (μ) of the undoped and Nd-doped Cu_2O thin films

Table 3 Electrical properties of Nd doped copper oxide thin films

Nd doping (%) in Cu_2O	Resistivity (Ω cm) $\times 10^2$	Carrier concentration (cm^{-3}) $\times 10^{15}$	Hall mobility cm^2/V s	Conductivity ($1/\Omega$ cm) $\times 10^{-3}$
0	1.85	17.94	1.88	5.40
1	1.61	18.82	2.06	6.21
3	1.12	20.19	2.76	8.92
5	0.85	21.66	3.39	11.76

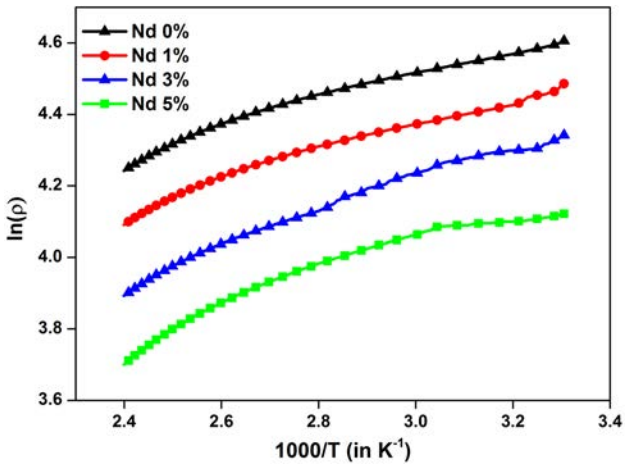

Fig. 12 Arrhenius plot of undoped and Nd-doped Cu_2O thin films

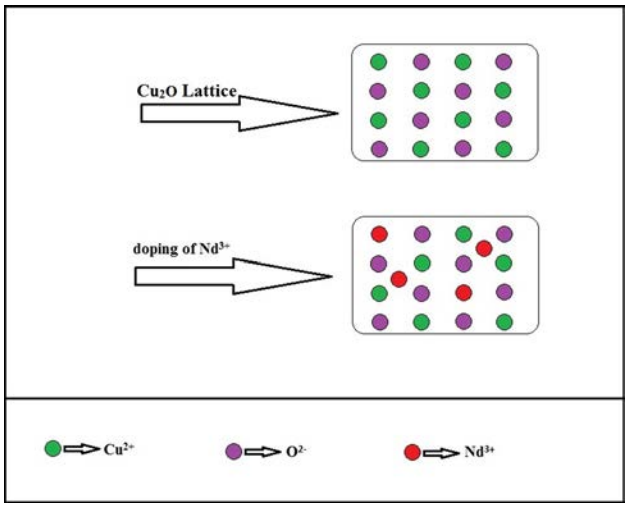

Fig. 13 Possible mechanism of Nd^{3+} ions in Cu_2O lattice

doped Cu_2O thin films is equal to that of the previous reports of Cu_2O [33, 34]. The Fig. 12 shows the graph of resistivity with inverse temperature. The resistivity of the film decreases by increasing the Nd doping % with the increase of temperature. The low resistivity values were found for the film deposited with the Nd 5% doping. The variation of temperature depended resistivity was well matching with the obtained room temperature Hall effect resistivity. The temperature having a good effect on the deposited Nd doped Cu_2O thin films as conductivity increases by increasing the temperature which shows the semiconducting behaviour of the films.

The Fig. 13 shows the possible mechanism of Nd^{3+} ions act in Cu_2O lattice. The low resistivity is found for the film deposited with 5% Nd doping with Cu_2O. Nd^{3+} ions were

interstitial position near the Cu sites in the Cu_2O lattice. The possible mechanism is, the incorporation of Nd^{3+} ions can create few free electrons and enhance the electrical properties. The conductivity increases with the increase of Nd doping which attributed to the Nd^{3+} ions occupying the copper vacancies.

3.6 Solar cell studies

The fabricated solar cell has the structure of glass substrate/FTO/ZnO/un-doped and Nd doped Cu_2O. In order to check the photovoltaic activity of the prepared solar cell the I–V measurements were analyzed at room temperature under the illumination at 200 W/m^2 halogen lamp. The solar cell active area was 0.5 cm^2. Figure 14 shows the illuminated I–V characteristics of ZnO-undoped and Nd doped Cu_2O heterojunction thin films. The open circuit voltage (V_{oc}) and short circuit current (I_{sc}) were determined from the I–V graph which shown that the current levels increased for the increasing of Nd doping % in Cu_2O films, in an illuminated conditions. The calculated solar cell parameters V_{oc}, I_{sc}, are presented in Table 4. The open circuit voltages (V_{oc}) were 0.25, 0.27, 0.34 and 0.39 V and short circuit currents (I_{sc}) were 1.2423×10^{-4}, 1.2892×10^{-4}, 1.3279×10^{-4} and 1.3867×10^{-4} A for different doping %. The improvement in short circuit current (I_{sc}) at increasing doping % might be due to the decrease of band gap and improvement of electrical properties at higher Nd doping % [35]. The fill factor and efficiency were calculated as per previous reports [36, 37].

Figure 15 shows the semi-log I-V graph of the heterojunction solar cells. The fill factor (FF) values were found to be 0.37, 0.38, 0.39 and 0.40 for the 0, 1, 3 and 5% of Nd concentration, respectively and the power conversion efficiencies 0.45, 0.51, 0.74 and 0.83% for the 0, 1, 3 and 5% Nd doped Cu_2O thin films. The obtained conversion efficiency is lower than the reported value of Cu_2O/ZnO heterojunction by Tanaka who obtained efficiency (η) of 1.2% [31]. To improve the solar cell performances the parameters like temperature, pressure, solution volume, concentration and doping with some other rare earth materials like Eu, Gd, Sr will be done in future.

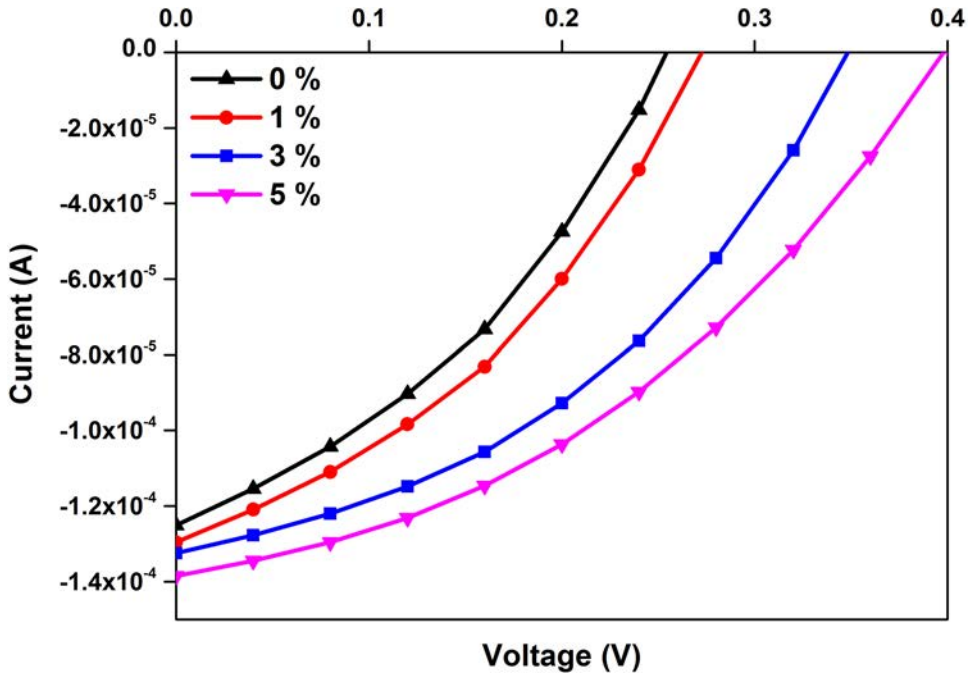

Fig. 14 Illuminated I–V characteristics of ZnO–Nd doped Cu_2O heterojunction thin films for different doping concentrations

Table 4 Photovoltaic parameters of ZnO/Cu_2O heterojunction solar cells

Nd doping (%) in Cu_2O	Open-circuit voltage V_{oc} (V)	Short circuit current density I_{sc} (mA)$\times10^{-4}$	Fill factor (FF) (%)	Efficiency η (%)
0	0.25	1.2423	0.37	0.45
1	0.27	1.2892	0.38	0.52
3	0.34	1.3279	0.39	0.70
5	0.39	1.3867	0.40	0.86

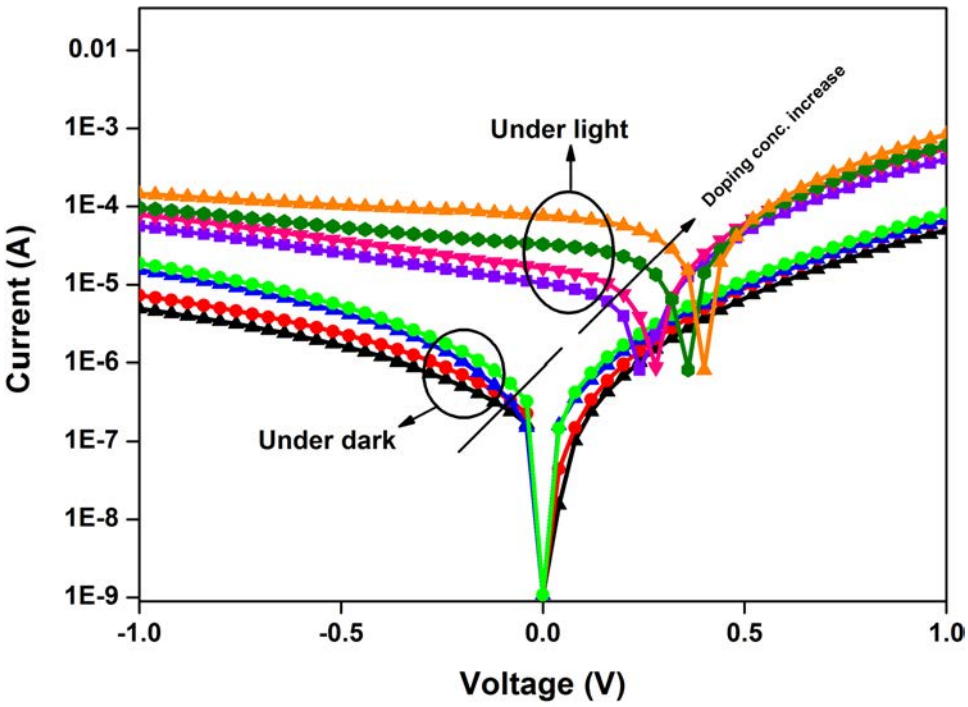

Fig. 15 Semi log I–V plot of the fabricated ZnO–Nd:Cu_2O solar cells

4 Conclusion

The undoped and 1, 3 and 5% of Nd doped copper oxide thin films were successfully deposited by using nebulizer spray pyrolysis. The X-ray diffraction studies conformed the Cu_2O phase with polycrystalline nature having cubic crystal structure for the prepared film and were matched with the standard JCPDS (Card No: 77-0199). The calculated crystallite size of the Cu_2O thin films are 36, 34, 28, and 23 nm respectively for the 0, 1, 3 and 5% of Nd doping. The optical band gap decreased from 2 to 1.82 eV on increasing the Nd doping %. The PL spectra peak at 617 nm was most likely attributable to acceptor-related luminescence, taking account of the band gap energy of Cu_2O. The resistivity of the film decreased from 1.85 to 0.85×10^2 Ω cm by increasing the doping content. Power conversion efficiencies 0.45, 0.51, 0.74 and 0.83% for the 0, 1, 3 and 5% Nd doped Cu_2O thin films were obtained in ZnO/Nd:Cu_2O hetrostructure solar cells.

Acknowledgements This work was supported by DST, India, under the scheme of Science and Engineering Research Board (SERB). DST. No. SB/FTP/PS-131/2013.

Compliance with ethical standards

Conflict of interest Authors declares that there is no conflict of interest in the current article.

References

1. B. Balamurunga, B.R. Mehta, Thin Solid Films **396**, 90 (2001)
2. A.E. Rakshani, Solid-State Electron. **29**, 7 (1986)
3. N.J. Gerein, J.A. Haber, J. Phys. Chem. B **109**, 17372–17385 (2005)
4. K. Santra, C.K. Sarkar, M.K. Mukherjee, B. Ghosh, Thin Solid Films **213**, 226 (1992)
5. T. Maruyama, Sol. Energy Mater. Sol. Cells **56**, 85–92 (1998)
6. Y.S. Gong, C. Lee, C.K. Yang, J. Appl. Phys. **77**, 5422 (1995)
7. V.F. Drobny, D.L. Pulfrey, Thin Solid Films **61**, 89 (1979)
8. A.Y. Oral, E. Mensur, M.H. Aslan, E. Basaran, Mater. Chem. Phys. **83**, 140 (2004)
9. M. Parhizkar, N. Kumar, P.K. Nayak, S. Singh, S.S. Tal-war, S.S. Major, R.S. Srinivasa, J. Colloids Surf. A **257**, 445 (2005)
10. P. Karthik, D. Vijayanarayanan, S. Suja, M. Sridharan, K. Jeyadheepan, Asian J Appl. Sci. **8**, 259–268 (2015)
11. Y. Chen, L. Yang, C. Feng, L.P. Wen, Biochem. Biophys. Res. Commun. **337**, 52–60 (2005)
12. I. Kostova, R. Kostova, G. Momekov, N. Trendafilova, M. Karaivanova, J. Trace Elem. Med. Biol. **18**, 219–226 (2005)
13. R. David Prabu, S. Valanarasu, J. Mater. Sci.: Mater. Electron. **28**, 6754–6762 (2017)
14. W.-H. Lan, C.-W. Tsai, S.-Y. Lee et al., Opto-Electron. Commun. 669–670 (2012)
15. T. Kosugi, S. Kaneko, J. Am. Ceram. Soc. **81**, 3117–3124 (1998)
16. R. David Prabu, S. Valanarasu., Mater. Sci. Semicond. Process. **74**, 129–135 (2018)
17. R. David Prabu, S. Valanarasu, Surf. Interface Anal. **50**, 346–353 (2018)
18. P.H. Klug, L.E. Alexander, *X-ray Diffraction Producers* (Wiley, New York, 1954)

19. M.R. Mariappan, V. Ponnuswamy Ragavendar, J. Alloys Compd. **509**, 7337–7343 (2011)
20. C.S. Barret, T.B. Massalski, *Structure of Metals*, vol. 204, 3rd edn. (Pergamon, Oxford, 1980)
21. H. Nagai, T. Suzuki et al., Mater. Chem. Phys. **137**, 252–257 (2012)
22. N. Choudhury, B.K. Sarma, Bull. Mater. Sci. **32**, 43–47 (2009)
23. M.A. Khan, M. Ullah et.al., Nanosci. Nanotechnol. Res. **3**, 16–22 (2015)
24. A. Ogwu, T. Darma, E. Bouquerel, J. Achiev. Mater. Manuf. Eng. **24**, 172–177 (2007)
25. K. Deva Arun Kumar, S. Valanarasu et.al., J. Electron. Mater. **28**, 14209–14216 (2017)
26. D. Sumangala, D. Amma, V.K. Vaidyan, P.K. Manoj et.al., Mater. Chem. Phys. **93**, 194–201 (2005)
27. A.M.S. Arulanantham, S. Valanarasu, J. Mater. Sci.: Mater. Electron. **28**, 1–11 (2017)
28. C. Vijayan, M. Pandiaraman, N. Soundararajan, R. Chandramohan, V. Dhanasekaran, K. Sundaram, T. Mahalingam, J. Peter, J. Mater. Sci. Mater. Electron. **22**, 545 (2011)
29. Y. Okamoto, S. Ishizuka, S. Kato, T. Sakurai, Appl. Phy. Lett. **82**, 7–17 (2003)
30. H. Nishikawa, T. Shiroyama, R. Nakamura, Y. Ohki, K. Nagasawa et al., Phys. Rev. B **45**, 586–591 (1992)
31. H. Tanaka, T. Shimakawa, T. Miyata, H. Sato, Minami, Thin Solid Films **469**, 80–85 (2004)
32. W.-H. Lan, C.-W. Tsai et al., in *Proceedings of the 17th Opto-Electronics and Communications Conference*, 2012, pp. 669–670
33. E. Fortin, F.L. Weichman, Can. J. Phys. **44**, 1551 (1966)
34. G.P. Pollack, D. Trivich, J. Appl. Phys. **46**, 163 (1975)
35. S. Jung, S. Ahn, J.H. Yun, J. Gwak, D. Kim, K. Yoon, Curr. Appl. Phys. **10**, 990–996 (2010)
36. T. Coutts, Thin film solar cells. Thin Solid Films **50**, 99–117 (1978)
37. V.D. Das, L. Damodare, J. Appl. Phys. **81**, 1522–1530 (1997)